

Cite this: *Chem. Sci.*, 2018, **9**, 3881

A redox-active diborane platform performs C(sp³)–H activation and nucleophilic substitution reactions†

Thomas Kaese, Timo Trageser, Hendrik Budz, Michael Bolte, Hans-Wolfram Lerner and Matthias Wagner *

Organoboranes are among the most versatile and widely used reagents in synthetic chemistry. A significant further expansion of their application spectrum would be achievable if boron-containing reactive intermediates capable of inserting into C–H bonds or performing nucleophilic substitution reactions were readily available. However, current progress in the field is still hampered by a lack of universal design concepts and mechanistic understanding. Herein we report that the doubly arylene-bridged diborane(6) 1H_2 and its B=B-bonded formal deprotonation product $\text{Li}_2[1]$ can activate the particularly inert C(sp³)–H bonds of added H_3ClLi and H_3CCl , respectively. The first case involves the attack of $[\text{H}_3\text{Cl}]^-$ on a Lewis-acidic boron center, whereas the second case follows a polarity-inverted pathway with nucleophilic attack of the B=B double bond on H_3CCl . Mechanistic details were elucidated by means of deuterium-labeled reagents, a radical clock, α,ω -dihaloalkane substrates, the experimental identification of key intermediates, and quantum-chemical calculations. It turned out that both systems, $\text{H}_3\text{ClLi}/1\text{H}_2$ and $\text{H}_3\text{CCl}/\text{Li}_2[1]$, ultimately funnel into the same reaction pathway, which likely proceeds past a borylene-type intermediate and requires the cooperative interaction of both boron atoms.

Received 13th February 2018
Accepted 19th March 2018

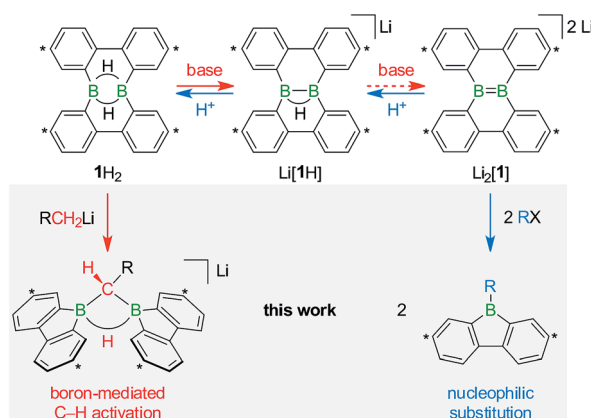
DOI: 10.1039/c8sc00743h
rsc.li/chemical-science

Introduction

For decades, organoboranes remained limited to a passive role as reagents in organic synthesis, where boryl substituents either serve as placeholders for other functional groups (*e.g.*, halides, hydroxy, and amino groups),¹ or are involved in Pd-catalyzed C–C-coupling reactions.² Another useful asset, the potential of boron compounds to actively promote the cleavage of element–element bonds, lay dormant until the concepts of “Boron Lewis-acid catalysis”^{3–6} and “Frustrated Lewis pairs”^{7–9} were introduced about 15 years ago. Since then, it became increasingly apparent that appropriately selected main group compounds can rival transition metal complexes in mediating the transformation of organic substrates.

Certain organoboranes are catalytically active not only in their Lewis-acidic neutral forms, but also in their exhaustively reduced states. As prominent examples, 9,10-dihydro-9,10-diboraanthracenes (DBAs) catalyze inverse electron-demand Diels–Alder reactions of 1,2-diazines³ as well as the dehydrogenation of ammonia-borane.⁵ Upon reduction, the

corresponding [DBA]^{2–} anions readily add C(sp³)–H or H–H bonds across the two boron atoms; the latter reaction can be exploited for the economic conversion of chlorosilanes into hydrosilanes.^{10,11}



Scheme 1 The members of the triad $1\text{H}_2/\text{Li}[1\text{H}]/\text{Li}_2[1]$ are linked through redox processes as well as protonation/deprotonation reactions. Treatment of 1H_2 with RCH_2Li leads to C(sp³)–H activations and skeletal rearrangements to furnish 1,1-bis(9-borafluorenyl)methanes (together with $\text{Li}[1\text{H}]$; $\text{R} = \text{H}, \text{C}_5\text{H}_7$). The addition of haloalkanes RX to $\text{Li}_2[1]$ results in nucleophilic substitution reactions and again skeletal rearrangements to afford 9- R -9-borafluorenes (in some cases accompanied by C(sp³)–H activations; $\text{X} = \text{Cl}, \text{Br}, \text{I}$). Carbon atoms marked with asterisks bear tBu substituents.

Institut für Anorganische und Analytische Chemie, Goethe-Universität Frankfurt, Max-von-Laue-Straße 7, D-60438 Frankfurt am Main, Germany. E-mail: matthias.wagner@chemie.uni-frankfurt.de

† Electronic supplementary information (ESI) available. CCDC 1819687–1819695. For ESI and crystallographic data in CIF or other electronic format see DOI: 10.1039/c8sc00743h



With the triad $\mathbf{1H}_2/\mathbf{Li}[\mathbf{1H}]/\mathbf{Li}_2[\mathbf{1}]$ (Scheme 1), we recently developed a system of ditopic boranes, which is comparable to the $\mathbf{DBA}/[\mathbf{DBA}]^{2-}$ pair, because it encompasses a Lewis-acidic ($\mathbf{1H}_2$) together with a dianionic species ($[\mathbf{1}]^{2-}$). As a decisive difference, however, the boron atoms in $[\mathbf{DBA}]^{2-}$ are linked by two *o*-phenylene rings, whereas in $[\mathbf{1}]^{2-}$ they are directly connected by a double bond. Both systems thus possess different frontier orbitals and should exhibit different reactivities.

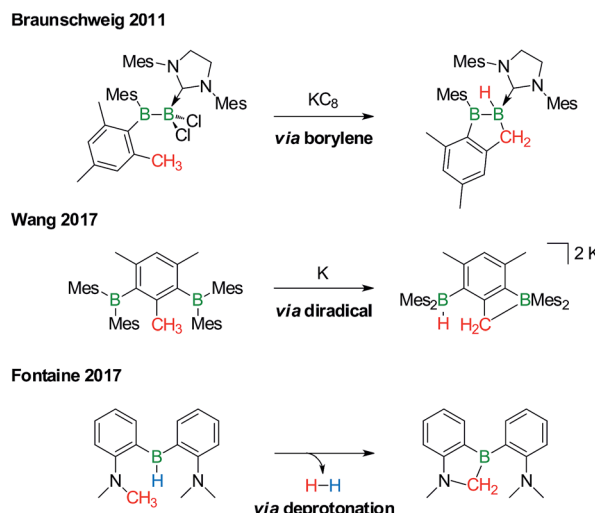
The anions $[\mathbf{1H}]^-$ and $[\mathbf{1}]^{2-}$ are accessible in good yields *via* alkali-metal reduction of $\mathbf{1H}_2$.¹²⁻¹⁴ Stepwise protonation with ethereal HCl cleanly takes $[\mathbf{1}]^{2-}$ back to $[\mathbf{1H}]^-$ and finally $\mathbf{1H}_2$.¹⁴ The reverse deprotonation reaction of $\mathbf{1H}_2$ to afford $[\mathbf{1H}]^-$ is also quantitative, provided that the sterically demanding bases $(\text{Me}_3\text{Si})_2\text{NLi}$ and $(\text{Me}_3\text{Si})_3\text{CLi}$ are used. In case of the smaller *n*BuLi, the deprotonation reaction (20%) is accompanied by the formation of an anionic diborylmethane featuring a boron-bridging hydrogen atom (30%; Scheme 1, R = C_3H_7).¹⁴ These remarkable results immediately raise the following questions: (i) can $\mathbf{1H}_2$ activate $\text{C}(\text{sp}^3)\text{-H}$ bonds of added alkylolithium reagents RCH_2Li ? (ii) Will $[\mathbf{1}]^{2-}$ show nucleophilic behavior also toward electrophiles other than the proton (*i.e.*, RX)?

Derivatization reactions of the inert $\text{C}(\text{sp}^3)\text{-H}$ bond are as topical as they are challenging – even if transition-metal catalysts are present.¹⁵⁻¹⁸ The few known boron-promoted examples fall into the three categories compiled in Scheme 2: (1) Braunschweig performed the reductive dechlorination of a dichloroborane precursor to generate an intermediate borylene, which inserted into the H_3C group of a nearby mesityl substituent.¹⁹ (2) Wang *et al.* observed hydrogen-atom abstraction from a H_3C group with concomitant formation of B-H and B-C bonds when they reduced 2,6-bis(BMes₂)mesitylene to its diradical state.²⁰ (3) Fontaine exploited an intramolecular deprotonation step on an FLP platform to establish an $\text{NCH}_2\text{-B}$ bond; subsequent H_2 liberation provided the necessary thermodynamic driving force.²¹

The umpolung of carbon electrophiles through their conversion in, *e.g.*, nucleophilic organolithium or Grignard reagents was one of the most important breakthroughs for the laboratory synthesis of organic compounds. A comparably high impact on the future progress of boron chemistry can be expected from the development of efficient tools to accomplish a polarity inversion of the intrinsically electrophilic boron center.²²

In 2006, Yamashita and Nozaki pioneered the field of nucleophilic boron compounds by disclosing a lithium boryl isostere of stable *N*-heterocyclic carbenes (NHCs; Fig. 1).²³ More than 10 years later, Hill expanded the class of compounds to include an isolable magnesium pinacolatoboryl complex.²⁴ In the intervening period, a wealth of chemistry had already been developed based on the *in situ* generation of pinacolatoboryl nucleophiles *via* the alkoxide-induced heterolytic cleavage of bis(pinacolato)diboron (Lin, Kleeberg, Marder and others).²⁵ Boryl nucleophiles can also be stabilized through π delocalization of the boron lone pair, as exemplified by Braunschweig's NHC-adduct of a borolyl salt (which may in fact react *via* radical pathways),²⁶ the cyclic (alkyl)(amino)carbene-coordinated BH fragment of Kinjo/Bertrand,²⁷ as well as Willner's/Finze's alkali metal tricyanoborate (Fig. 1).²⁸

Before the background provided by the literature and our own previous results, we regarded the triad $\mathbf{1H}_2/\mathbf{Li}[\mathbf{1H}]/\mathbf{Li}_2[\mathbf{1}]$ as a perfect platform for further studies into boron-promoted C-H-activation processes and boron-centered nucleophiles. Herein we present evidence that the reactions of $\mathbf{1H}_2$ with RCH_2Li indeed proceed through $\text{C}(\text{sp}^3)\text{-H}$ -cleavage steps and that the boron-bridging H atoms in the diborylmethane products stem from the organolithium reagents and are not remains of $\mathbf{1H}_2$ (*cf.* Scheme 1; R = H, C_3H_7). We also show that the B=B double bond of the dianion $[\mathbf{1}]^{2-}$ behaves as a closed-shell nucleophile toward organohalides and that specifically $\text{H}_3\text{CCl}/\mathbf{Li}_2[\mathbf{1}]$ and $\text{H}_3\text{CLi}/\mathbf{1H}_2$ funnel into the same reaction channel. When H_3CCl is replaced by an excess of $\text{H}_3\text{C-I}$, C-H-activation is completely suppressed by a second nucleophilic substitution reaction to afford 2 equiv. of 9-methyl-9-borafluorene (Scheme 1; R = H_3C). Employing α,ω -dihaloalkanes $\text{X}(\text{CH}_2)_n\text{X}$ and $\mathbf{Li}_2[\mathbf{1}]$, we gained



Scheme 2 Selected examples of transition metal-free intramolecular $\text{C}(\text{sp}^3)\text{-H}$ activations through borylene (top), diradical (middle), and deprotonation reactions (bottom). Mes = 2,4,6-(H_3C)₃ C_6H_2 .

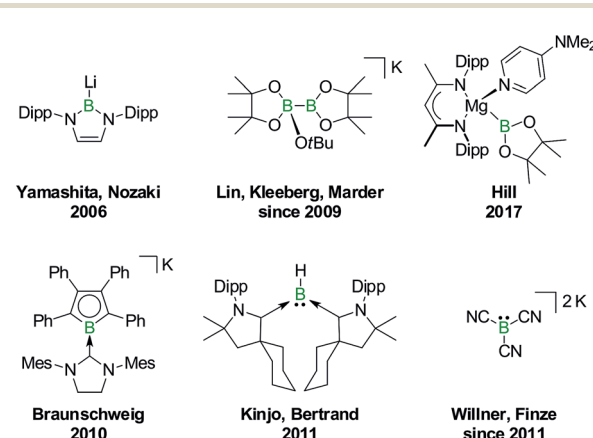


Fig. 1 Selected isolable boron compounds showing formal nucleophilic behavior. Dipp = 2,6-(*i*Pr)₂ C_6H_3 .



further insight into the competition between the nucleophilic substitution and C–H-activation scenarios as well as the cooperativity of the two adjacent boron centers ($X = \text{Cl}, \text{Br}$).

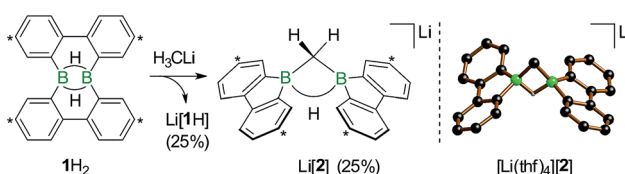
Results and discussion

We started our study by addressing the question: why and how does the reaction of **1H₂** with *n*BuLi furnish not only the deprotonation product Li[1H], but also the diborylmethane-hydride adduct shown in Scheme 1 ($\text{R} = \text{C}_3\text{H}_7$)?

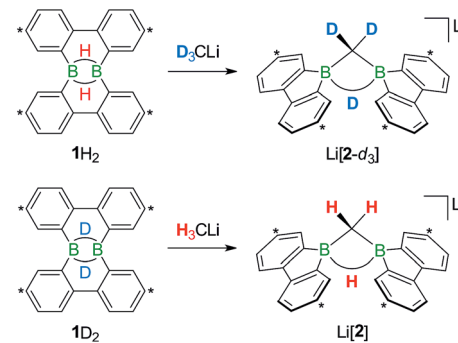
First, we confirmed that a simplified system using H₃CLI in place of *n*BuLi maintains the same general reactivity (Scheme 3). From equimolar mixtures of **1H₂** and H₃CLI, the products Li[1H] and Li[2] are formed in slightly varying relative amounts but constant combined yields of close to 50% (the analogous finding holds for the *n*BuLi case). The ¹H NMR spectroscopic monitoring of the reaction in a sealed NMR tube (THF-*d*₈, room temperature) showed no free H₂ (δ 4.55 ppm),²⁹ which is an important observation considering that the starting materials **1H₂** and H₃CLI contain a sum of five BHB/H₃CLI protons, of which only three remain in the product Li[2].

Deuterium-labeling experiments with D₃CLI/1H₂ or H₃CLI/1D₂ combinations furnished isotopically pure Li[2-*d*₃] or Li[2], respectively (Scheme 4). Thus, not only the methylene linker (δ ¹H 0.49 ppm, d), but also the boron-bridging hydrogen atom (δ ¹H 1.94 ppm, br) in Li[2] originate from the organolithium reagent. None of the two BHB atoms of **1H₂** is still present in the product Li[2-*d*₃] (see the ESI† for more information). We also note the appearance of two sets of aryl-proton signals that neither belong to Li[1H] nor Li[2] (or their partly deuterated counterparts) and are consequently accountable for the missing 50% product yield (see below).

In the following, a plausible mechanistic model for the conversion of **1H₂** with H₃CLI will be described (black arrows in Scheme 5), which accounts for all available experimental evidence. It explains (i) the C–H activation of [H₃C][–], (ii) the fate of the boron-bonded hydrogen atoms of **1H₂**, and (iii) the combined yield of only 50% for Li[1H] and Li[2]: similar to the case (Me₃Si)₃CLI/1H₂, the reaction H₃CLI/1H₂ starts with the deprotonation of **1H₂** to afford Li[1H]. The byproduct CH₄ was detected by ¹H and ¹³C{¹H} NMR spectroscopy; when D₃CLI was employed as the Brønsted base, we instead observed the



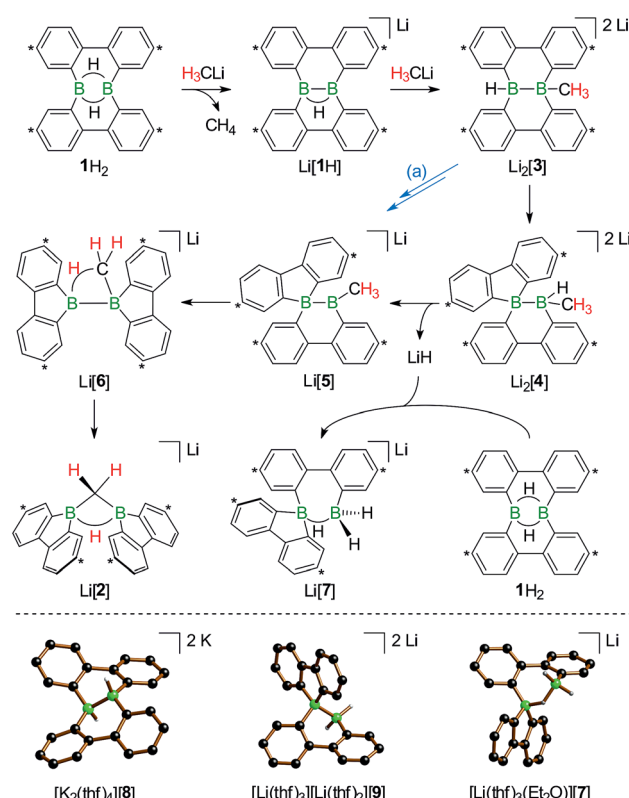
Scheme 3 The addition of H₃CLI to **1H₂** furnishes the C–H activation product Li[2] together with the deprotonated compound Li[1H] (left; carbon atoms marked with asterisks bear tBu substituents). Molecular structure of [Li(thf)₄]⁺[2] in the solid state (right). The solvent-separated [Li(thf)₄]⁺ cation, all tBu groups, and all CH atoms are omitted for clarity. Selected atom–atom distance [Å] and bond angle [°]: B–B = 1.974(6); B–CH₂–B = 76.8(3).



Scheme 4 The reactions D₃CLI/1H₂ (top) or H₃CLI/1D₂ (bottom) give the C–D- or C–H-activation products Li[2-*d*₃] or Li[2], respectively. Carbon atoms marked with asterisks bear tBu substituents.

formation of D₃CH (sealed NMR tubes; see the ESI† for more details).

Contrary to the case (Me₃Si)₃CLI/1H₂, the reaction involving H₃CLI does not necessarily stop at the stage of Li[1H], because the small [H₃C][–] ion also has the potential to act as a Lewis base. Nucleophilic attack of H₃CLI on a boron atom of Li[1H]



Scheme 5 Proposed reaction mechanism explaining the formation of Li[1H], Li[2], and Li[7] from an equimolar mixture of H₃CLI and 1H₂ (top; carbon atoms marked with asterisks bear tBu substituents). The alternative pathway (a) leads from Li₂[3] to Li[5], first via hydride elimination and second via a 1,2-phenyl shift. Molecular structures of [K₂(thf)₄]⁺[8], [Li(thf)₃]⁺[Li(thf)₂][–][9], and [Li(thf)₃(Et₂O)]⁺[7] in the solid state (bottom). The solvent-separated cations, all tBu groups, and all CH atoms are omitted for clarity.



establishes a B-CH₃ bond and shifts the boron-bridging hydrogen atom to a terminal position. The structural motif of the resulting intermediate [3]²⁻ has precedence in the crystallographically characterized dianion [8]²⁻,¹³ which carries a further hydrogen atom rather than a boron-bonded methyl group (Scheme 5, top and bottom). Li₂[3] rearranges to Li₂[4] through a 1,2-phenyl shift, accompanied by a 1,2-hydride shift. Again, a comparable hydrogen-containing species Li₂[9] exists (Scheme 5, bottom), and its molecular structure has been confirmed by X-ray analysis.¹³ Li₂[9] can isomerize to Li₂[FluB(H)-(H)BFlu] (BFlu = 9-borafluorenyl),¹³ thereby providing an example of a 1,2-phenyl/1,2-hydride-shift cascade closely related to the isomerization of Li₂[3] to Li₂[4]. The latter reaction continues with an LiH-elimination step to generate Li[5], which possesses a three-coordinate boron atom with a vacant p_z orbital and therefore easily undergoes a 1,2-phenyl shift to produce Li[6]. The anion [6]⁻ can be viewed as the [H₃C]⁻ adduct of a diborane(4) containing two 9-borafluorene units that are linked by a B-B single bond. Only the sp³-hybridized boron atom has acquired an electron octet, however, also the B(sp²) center might gain some electron density from an agostic interaction with the methyl group and thereby reduce its strong Lewis acidity.³⁰ Finally, this interaction turns into C-H-bond activation accompanied by B-B-bond cleavage and ultimately results in the formation of Li[2]. It is well known that B(sp²)-B(sp³) diboranes readily undergo B-B-bond heterolysis and thereby act as mild sources of nucleophilic boron.³¹ Moreover, the core parts of [2]⁻ and [6]⁻ are isoelectronic with protonated cyclopropane [C₃H₇]⁺. This cation has been thoroughly investigated by experimental³²⁻³⁴ and theoretical^{35,36} methods and found to be a highly fluctual system,³⁷ which supports the idea of [6]⁻ rearranging to [2]⁻. At this stage, the dynamic behavior comes to an end, because, contrary to the case of [C₃H₇]⁺, the three corners of [2]⁻ are not equivalent and the BHB bridge should be thermodynamically favored over alternative BHC bridges.

In addition to the qualitative comparison with the all-carbon model system [C₃H₇]⁺, we studied the key C-H-activation step of the organoboron anion [6]⁻ by quantum-chemical calculations (Fig. 2). Apart from the Li⁺ counterion, which likely is solvent-separated in THF solution (*cf.* the solid-state structure of [Li(thf)₄][2]; Scheme 3, right), we also omitted the *t*Bu substituents. The computed parent systems will be denoted with a superscript 'c' (e.g., [5^c]⁻ represents Li[5]). The 1,2-phenyl shift in [5^c]⁻ proceeds *via* TS1 with an activation barrier of $\Delta G^\ddagger = 9.9$ kcal mol⁻¹ and is endoergic by $\Delta G_R = 5.9$ kcal mol⁻¹. The resulting open-chain rearrangement product [6^c-open]⁻ features a large B-B-CH₃ bond angle of 121° and the vacant p_z orbital of the B(sp²) atom is oriented almost orthogonal to the B-CH₃-bond vector, which precludes an agostic interaction in this isomer. To establish the B-H-C bridge proposed above, the tricoordinate borafluorene fragment must be rotated by approximately 70° and the B-B-CH₃ bond angle contracted – ultimately to a value of 68° in the local-minimum structure [6^c]⁻. The conversion of [6^c-open]⁻ to the cyclic isomer [6^c]⁻ *via* TS2 ($\Delta G^\ddagger = 7.0$ kcal mol⁻¹) is associated with a moderate energy penalty of $\Delta G_R = 4.6$ kcal mol⁻¹. The actual C-H-activation process involves the transition state TS3 in which the B-B bond and one C-H bond are concertedly cleaved and a new B-C bond is formed ($\Delta G^\ddagger = 4.4$ kcal mol⁻¹).

The primary, open-chain activation product [2^c-open]⁻ is thermodynamically favored by -14.1 kcal mol⁻¹ and -3.6 kcal mol⁻¹ compared to [6^c]⁻ and [5^c]⁻, respectively. A further stabilization is achievable through rotation about a B-C bond and placement of the hydrogen atom into a boron-bridging position to obtain the final product [2^c]⁻ (TS4: $\Delta G^\ddagger = 2.7$ kcal mol⁻¹; $\Delta G_R = -6.3$ kcal mol⁻¹). In summary, the reaction cascade from [5^c]⁻ to [2^c]⁻ possesses an overall activation barrier of $\Delta G^\ddagger = 14.9$ kcal mol⁻¹, which is easily surmountable at room temperature. An appreciable thermodynamic driving force is provided by the exergonicity of the [2^c]⁻ formation ($\Delta G_R = -9.9$ kcal mol⁻¹).

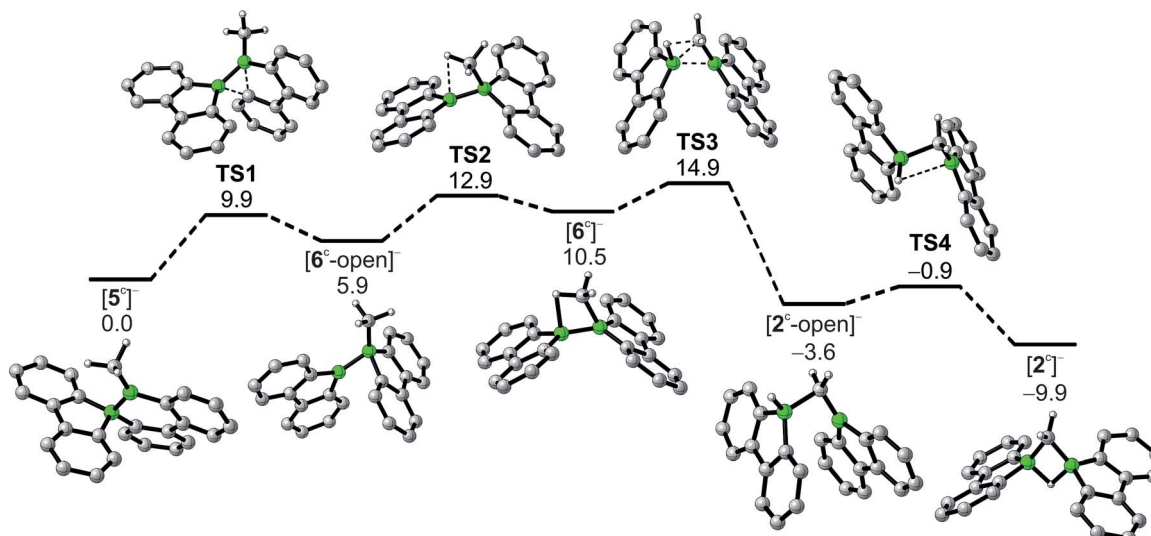


Fig. 2 Reaction pathway for the conversion of [5^c]⁻ to [2^c]⁻, calculated at the PBE0D/TZVP level of theory with the SMD polarized continuum model for solvation in THF. Gibbs free energies at 298 K (ΔG) are given in kcal mol⁻¹ relative to [5^c]⁻.



To experimentally substantiate the role of $\text{Li}[1\text{H}]$ as the first intermediate along the pathway from $\mathbf{1H}_2$ to $\mathbf{Li}[2]$, we treated an isolated sample of $\mathbf{Li}[1\text{H}]$ with 1 equiv. of H_3CLi in THF. Even though the reaction started as expected, it stopped at the stage of $\text{Li}_2[\mathbf{4}]$ (which enabled us to record a ^1H NMR spectrum of this compound). The elimination of LiH from $\text{Li}_2[\mathbf{4}]$ is thus not a spontaneous process, but apparently requires a hydride-trapping reagent. Compound $\mathbf{1H}_2$ constitutes an ideal candidate for this purpose and, indeed, after the addition of 1 equiv. of $\mathbf{1H}_2$, $\text{Li}_2[\mathbf{4}]$ quantitatively vanished and $\mathbf{Li}[2]$ formed instead. Moreover, we found two sets of proton resonances that are assignable to two isomeric hydride-trapping products of $\mathbf{1H}_2$ (*cf.* $\mathbf{Li}[7]$, $\mathbf{Li}[10]$; Schemes 5 and 6).

As a caveat we emphasize that the reaction from $\mathbf{1H}_2$ to $\mathbf{Li}[2]$ may bypass the intermediate $\mathbf{Li}_2[\mathbf{4}]$ if hydride transfer from $\mathbf{Li}_2[\mathbf{3}]$ to $\mathbf{1H}_2$ is faster than the rearrangement from $\mathbf{Li}_2[\mathbf{3}]$ to $\mathbf{Li}_2[\mathbf{4}]$ (blue path (a) in Scheme 5). Arguments in favor of this alternative route include: (i) the 1,2-phenyl shift required to generate intermediate $\mathbf{Li}[5]$ should be more facile on a $\text{B}(\text{sp}^2)\text{-B}(\text{sp}^3)$ rather than a $\text{B}(\text{sp}^3)\text{-B}(\text{sp}^3)$ scaffold (*cf.* $\mathbf{Li}_2[\mathbf{3}] \rightarrow \mathbf{Li}_2[\mathbf{4}]$; Scheme 5). (ii) $\mathbf{Li}_2[\mathbf{4}]$ was observed only when the reaction was started from $\mathbf{Li}[1\text{H}]$, *i.e.*, when the hydride trap $\mathbf{1H}_2$ was absent, thus rendering the blue path impassable.

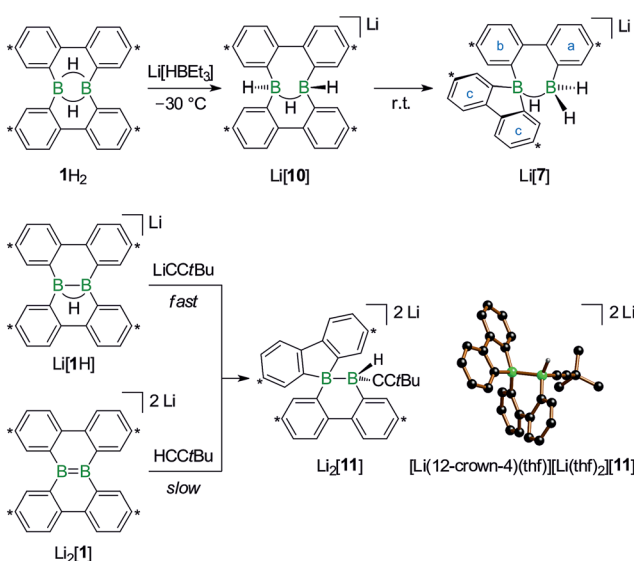
After the above discussion of a plausible mechanistic picture underlying the overall reaction scenario, we now present analytical data of key intermediates and products. The reaction $\text{H}_3\text{CLi}/\mathbf{1H}_2$ furnishes $\mathbf{Li}[1\text{H}]$ and $\mathbf{Li}[2]$ besides the isomeric hydride-trapping products $\mathbf{Li}[7]$ and $\mathbf{Li}[10]$. The first species, $\mathbf{Li}[1\text{H}]$, is a known compound and therefore does not require further discussion.¹⁴ The second species, $\mathbf{Li}[2]$, is reminiscent of

the published C–H-activation product obtained from the reaction $n\text{BuLi}/\mathbf{1H}_2$ (*cf.* Scheme 1, $\text{R} = \text{C}_3\text{H}_7$).¹⁴ The main difference between both compounds relates to the fact that $\mathbf{Li}[2]$ possesses an average C_{2v} symmetry in solution, whereas a pending C_3H_7 substituent reduces the symmetry to C_s . Consequently, the ^1H NMR spectrum of $\mathbf{Li}[2]$ contains only one set of signals for all four $t\text{Bu-C}_6\text{H}_3$ rings. The corresponding spectrum of its C_s -symmetric congener features two sets of resonances,¹⁴ one of them with chemical shift values almost identical to those of $\mathbf{Li}[2]$ and thus likely assignable to those halves of the 9-borafluorene subunits, which point into the same direction as the proton residing on the methylene bridge. A similar interpretation is valid for the $^{13}\text{C}[^1\text{H}]$ NMR spectrum of $\mathbf{Li}[2]$. Single crystals of $[\text{Li}(\text{thf})_4][2]$ suitable for X-ray analysis were grown from THF-hexane (Scheme 3). Like its C_3H_7 derivative,¹⁴ $[\text{Li}(\text{thf})_4][2]$ forms solvent-separated ion pairs in the crystal lattice, and all key geometric parameters of the two anions are identical within the experimental error margins. We also note a pleasingly good agreement between the experimentally determined structure of $[2]^-$ and the computed structure of $[2]^-$ (*cf.* the ESI† for full details).

^1H NMR spectra measured on $\text{H}_3\text{CLi}/\mathbf{1H}_2$ mixtures reproducibly showed resonances pointing toward a primary hydride-trapping product $\mathbf{Li}[10]$, which features a BHB bridge and two terminal hydrogen substituents in mutual *trans* arrangement (Scheme 6). For comparison, we prepared an authentic sample of $\mathbf{Li}[10]$ from $\mathbf{1H}_2$ and 1 equiv. of the ‘superhydride’ $\text{Li}[\text{HBET}_3]$. At low temperatures, $\mathbf{Li}[10]$ forms quantitatively; since the compound is thermolabile, its NMR spectra had to be recorded at $-30\text{ }^\circ\text{C}$. $\mathbf{Li}[10]$ gives rise to a double set of proton resonances in THF solution. On average, the two 2,2'-biphenylene fragments of the anion $[10]^-$ should be related by a mirror plane containing the B_2H_3 core. The two phenylene rings of each individual 2,2'-biphenylene moiety, however, are chemically inequivalent (as confirmed by 2D NMR experiments).

At room temperature, $\mathbf{Li}[10]$ readily isomerizes to the secondary hydride-trapping product $\mathbf{Li}[7]$, which we have isolated and characterized by NMR spectroscopy as well as X-ray crystallography. The anion of $[\text{Li}(\text{thf})_3(\text{Et}_2\text{O})][7]$ consists of one 9-borafluorenyl and one BH_2 fragment that are linked by a $\mu\text{-H}$ atom and a 2,2'-biphenylene bridge (Scheme 5, bottom). As a result, both boron atoms are tetracoordinate and placed at a distance of $\text{B}\cdots\text{B} = 2.382(8)\text{ \AA}$. In the solid state, the central seven-membered HB_2C_4 ring is non-planar and the anion possesses C_1 symmetry (the torsion angle of the bridging 2,2'-biphenylene amounts to 36°).

The molecular scaffolds of $[7]^-$ and the known anion $[9]^{2-}$ are essentially superimposable, apart from the fact that the latter features a covalent B–B bond ($1.810(5)\text{ \AA}$) instead of the $\mu\text{-H}$ atom (Scheme 5, bottom).¹³ In line with their marked structural resemblance, both anions exhibit similar ^1H NMR spectra: in each case, three sets of aryl resonances are detectable. Two of those are well resolved at room temperature (H-a, H-b), whereas the third set consists of very broad signals, each of them integrating 2H (H-c; Scheme 6). This points toward a dynamic behavior of the compounds in solution, which likely arises from conformational changes of the twisted boron heterocycles. The



Scheme 6 Reaction of $\mathbf{1H}_2$ with $\text{Li}[\text{HBET}_3]$ at $-30\text{ }^\circ\text{C}$ to give $\mathbf{Li}[10]$, which isomerizes to $\mathbf{Li}[7]$ at room temperature (top). Compound $\text{Li}_2[\mathbf{11}]$ forms in both reactions, $t\text{BuCClLi}/\mathbf{Li}[1\text{H}]$ and $t\text{BuCClH}/\mathbf{Li}_2[\mathbf{11}]$ (bottom; carbon atoms marked with asterisks bear $t\text{Bu}$ substituents). Molecular structure of $[\text{Li}(12\text{-crown-4})(\text{thf})][\text{Li}(\text{thf})_2][\mathbf{11}]$ in the solid state. The solvent-separated cations, phenyl-bonded $t\text{Bu}$ groups, and all CH atoms are omitted for clarity.



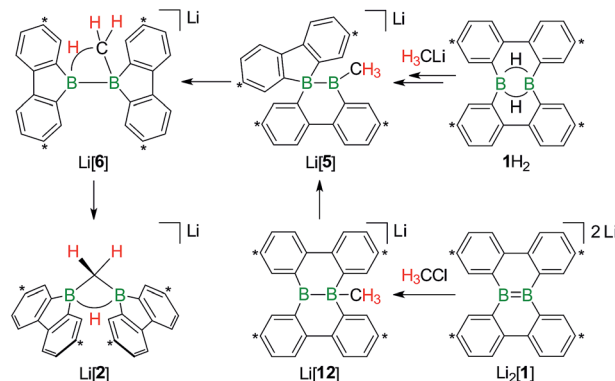
^{11}B NMR spectrum of $[\mathbf{7}]^-$ is characterized by two resonances with chemical shift values of $\delta = -3.6$ and -10.1 ppm, testifying to the presence of two magnetically inequivalent, tetracoordinate boron nuclei.³⁸

Turning our attention from the products of the reaction $\text{CH}_3\text{Li}/\text{H}_2$ to its intermediates, we note that the ^1H NMR spectrum of $\text{Li}_2[\mathbf{4}]$ shows the same peculiarities as those of its structural congeners $\text{Li}[\mathbf{7}]$ and $\text{Li}_2[\mathbf{9}]$: well resolved resonances coexist with severely broadened signals. Together with a BCH_3 resonance at $\delta = -0.1$ ppm, this can be taken as a support for our structural proposal of $\text{Li}_2[\mathbf{4}]$, but the motional broadening precludes the measurement of meaningful $^{13}\text{C}\{^1\text{H}\}$ NMR and 2D correlation spectra. Despite numerous efforts, we have not succeeded in growing crystals of $\text{Li}_2[\mathbf{4}]$ and therefore considered replacing the H_3C group with an alternative sterically undemanding organic substituent: The reaction $t\text{BuCCLi}/\text{Li}[\mathbf{1H}]$ provided the alkynyl analogue $\text{Li}_2[\mathbf{11}]$ of $\text{Li}_2[\mathbf{4}]$ in single-crystalline form ($[\text{Li}(12\text{-crown-4})(\text{thf})_2][\text{Li}(\text{thf})_2]\mathbf{11}$; Scheme 6). X-ray crystallography confirmed the proposed ring-contracted, H-shifted structure of $[\mathbf{11}]^{2-}$.

NMR spectroscopy reproduced the characteristic distribution of well-resolved and motionally broadened line shapes; the chemical shift values of the aryl protons of $\text{Li}_2[\mathbf{11}]$ are reasonably close to those of $\text{Li}_2[\mathbf{4}]$ (cf. the ESI† for an overlay of the respective ^1H NMR spectra). Remarkably, $\text{Li}_2[\mathbf{11}]$ is also accessible *via* a different approach, starting from the doubly boron-doped dibenzo[*g,p*]chrysene $\text{Li}_2[\mathbf{1}]$ and $t\text{BuCCH}$, the conjugate weak acid of $[t\text{BuCC}]^-$ (Scheme 6).

The facile protonation¹⁴ of $\text{Li}_2[\mathbf{1}]$ prompted us to investigate whether an umpolung approach to synthesize compounds of the type $\text{Li}[\mathbf{2}]$ might also be successful, which would provide fundamentally interesting insights into the reactivities of $\text{B}=\text{B}$ double-bonded species. As mentioned above, the intermediate $\text{Li}[\mathbf{6}]$ of the reaction $\text{H}_3\text{CLI}/\text{H}_2$ can be regarded as the $[\text{H}_3\text{C}]^-$ adduct of a diborane(4). Conceptually, it should be possible to arrive at the same molecule by formally transferring two electrons from the carbon nucleophile to the redox-active organoborane and thus starting from methyllium-ion sources and the anion $[\mathbf{1}]^{2-}$ (Fig. 3).³⁹

Indeed, when a THF solution of $\text{Li}_2[\mathbf{1}]$ is stirred at room temperature under a blanket of H_3CCl gas (1 atm), a quantitative conversion to $\text{Li}[\mathbf{2}]$ occurs (Scheme 7).⁴⁰ This approach is far more atom- and time-economic than the previous access route *via* the polarity-inverted couple $\text{H}_3\text{CLI}/\text{H}_2$, because we avoid wasting 50% of $\mathbf{1H}_2$ as a hydride-trapping reagent and do no



Scheme 7 The addition of H_3CCl to $\text{Li}_2[\mathbf{1}]$ quantitatively furnishes $\text{Li}[\mathbf{2}]$. The reaction pathways to $\text{Li}[\mathbf{2}]$, starting from either $\mathbf{1H}_2$ or $\text{Li}_2[\mathbf{1}]$, merge at the stage of $\text{Li}[\mathbf{5}]$ (cf. also Scheme 5). Carbon atoms marked with asterisks bear tBu substituents.

longer have to separate the resulting hydride-trapping products. Mechanistically, the electron-rich $\text{B}=\text{B}$ fragment of $\text{Li}_2[\mathbf{1}]$ likely acts as a nucleophile toward H_3CCl to form $[\mathbf{12}]^-$, which carries a boron-bonded methyl substituent and contains a central $\text{B}=\text{B}$ single bond. The $\text{B}(\text{sp}^2)-\text{B}(\text{sp}^3)$ species $\text{Li}[\mathbf{12}]$ then undergoes a 1,2-phenyl shift to afford $\text{Li}[\mathbf{5}]$ and thereby funnels into the reaction cascade outlined above for the formation of $\text{Li}[\mathbf{2}]$ from $\text{H}_3\text{CLI}/\text{H}_2$ (Scheme 7).

When H_3CCl is replaced by 1 equiv. of iodomethane ($\text{H}_3\text{C-I}$), the outcome is a mixture of $\text{Li}[\mathbf{2}]$, 9-methyl-9-borafluorene ($\mathbf{13}$), and residual $\text{Li}_2[\mathbf{1}]$ (Scheme 8). After increasing the relative amount of $\text{H}_3\text{C-I}$ to 3 equiv., we almost exclusively obtained $\mathbf{13}$. The different behaviors of the two halomethanes can be rationalized by viewing the intermediate $\text{Li}[\mathbf{6}]$ as an adduct between the 9-borafluorenyl anion ($[\text{BFu}]^-$) and $(\text{H}_3\text{C})\text{BFu}$ ($\mathbf{13}$; Scheme 9). $[\text{BFu}]^-$ is isoelectronic to the carbene 9-fluorenylidene. A formal carbene-like reactivity is reflected by the intramolecular insertion of $[\text{BFu}]^-$ into the C–H bond of the 9-methyl-9-borafluorene moiety to afford $\text{Li}[\mathbf{2}]$. When the strong electrophile $\text{H}_3\text{C-I}$ with its excellent iodide leaving group is present, also the nucleophilic character of $[\text{BFu}]^-$ comes into play and opens a competing intermolecular pathway, which ultimately leads to $\mathbf{13}$. As the relative amount of $\text{H}_3\text{C-I}$ is increased, the substitution reaction becomes dominant (we note in passing that the reaction with $\text{H}_3\text{C-I}$ can alternatively be viewed as a carbene-like insertion of $[\text{BFu}]^-$ into the C–I bond with subsequent elimination of LiI).

In case of the system $\text{H}_3\text{C-I}/\text{Li}_2[\mathbf{1}]$, the methyl group initially gets attached to only one of the symmetry-related boron centers, but the other is equally important for the subsequent C–H-activation and nucleophilic substitution steps. The degree of $\text{B}=\text{B}$ cooperativity in $\text{Li}_2[\mathbf{1}]$ as well as the insertion *vs.* nucleophilic behavior of $[\text{BFu}]^-$ thus deserve a detailed assessment. To this end, we conducted a systematic study using $1:1$ mixtures of $\text{Li}_2[\mathbf{1}]$ and α,ω -dihaloalkanes $\text{X}(\text{CH}_2)_n\text{X}$ with chain lengths in the range of $n = 2-6$ and leaving groups of different qualities (e.g., $\text{X} = \text{Cl}, \text{Br}$). In these experiments, smaller alkylidene linkers are supposed to mimic higher local concentrations of the electrophile. As summarized in Scheme 8, clean

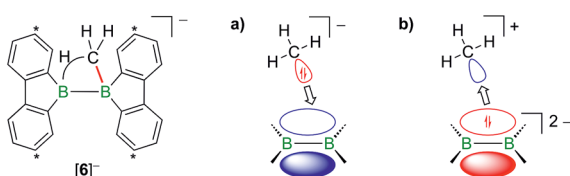
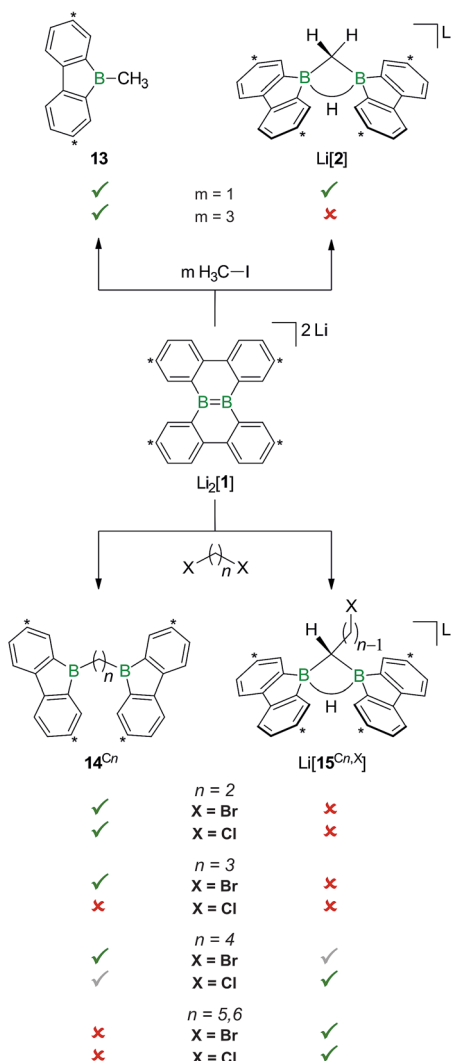


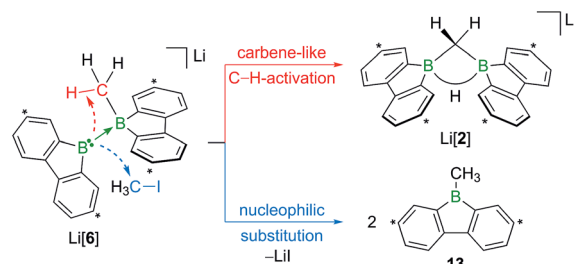
Fig. 3 Two borderline cases to describe the bonding situation in $[\mathbf{6}]^-$ as (a) the $[\text{H}_3\text{C}]^-$ adduct of a diborane(4) and (b) the $[\text{H}_3\text{C}]^+$ adduct of a $[\mathbf{1}]^{2-}$ anion. Carbon atoms marked with asterisks bear tBu substituents.





Scheme 8 The outcome of the reaction $\text{H}_3\text{C}-\text{I}/\text{Li}_2[1]$ depends on the stoichiometries employed. While 1 : 1 mixtures give **13** together with $\text{Li}[2]$, 3 : 1 mixtures exclusively furnish **13**. Use of α,ω -dihaloalkanes $\text{X}(\text{CH}_2)_n\text{X}$ instead of $\text{H}_3\text{C}-\text{I}$ affords ditopic boranes $\text{14}^{\text{C}n}$ ($n = 2-4$) and/or $\text{Li}[15^{\text{C}n,\text{X}}]$ ($n = 4-6$; $\text{X} = \text{Cl}, \text{Br}$). Carbon atoms marked with asterisks bear *t*Bu substituents.

twofold substitution reactions are observed with the short-chain substrates ($n = 2$ and 3, *cf.* **14**^{C₂} and **14**^{C₃}; 1,3-dichloropropane leads to a complex mixture of products). Clean C–H-activation reactions occur with the long-chain substrates ($n = 5$ and 6) to afford the haloalkyl species $\text{Li}[15^{\text{C}5,\text{Cl}}]/\text{Li}[15^{\text{C}5,\text{Br}}]$ and $\text{Li}[15^{\text{C}6,\text{Cl}}]/\text{Li}[15^{\text{C}6,\text{Br}}]$. The medium-chain substrates ($n = 4$) mark the switching point between both scenarios: with the worse chloride leaving group, C–H-activation is preferred over the twofold substitution. The reverse is true in the case of the better bromide leaving group. The solid-state structures of **14**^{C₂}·thf, **14**^{C₃} (Fig. 4), **14**^{C₄}, and $[\text{Li}(\text{12-crown-4})_2][15^{\text{C}5,\text{Cl}}]$ (Fig. 4) were characterized by X-ray crystallography (*cf.* the ESI† for full information). Also the connectivities of $[\text{Li}(\text{thf})_4][15^{\text{C}4,\text{Cl}}]$, $[\text{Li}(\text{thf})_4][15^{\text{C}6,\text{Cl}}]$, and $[\text{Li}(\text{thf})_4][15^{\text{C}6,\text{Br}}]$ are supported by X-ray diffraction studies, however, due to disordered haloalkyl



Scheme 9 The intermediate $\text{Li}[6]$ can be interpreted as an adduct between the 9-borafluorenyl anion ($[\text{BFlu}]^-$) and 9-methyl-9-borafluorene (**13**). Intramolecular C–H insertion of the carbene-like $[\text{BFlu}]^-$ furnishes $\text{Li}[2]$; intermolecular nucleophilic attack on $\text{H}_3\text{C}-\text{I}$ affords 2 equiv. of **13**. Carbon atoms marked with asterisks bear *t*Bu substituents.

chains, *t*Bu groups, and THF molecules, the quality of these three structures prevents their inclusion into this publication.⁴¹

The observed chain-length dependence of the product distribution suggests that the carbene-type insertion and the second nucleophilic substitution both follow an intramolecular pathway involving two cooperating boron atoms.

If the remaining CH_2X center and the BCH_2 group are similarly close to the B–B bond, the nucleophilic process occurs at a higher rate than the carbene-type C–H-activation. As the alkylidene spacer grows, the second electrophilic functionality moves further apart whereas the reactive α - CH_2 unit stays in place such that the C–H-activation becomes more and more relevant until it finally takes over.

Although the reaction between $\text{Li}_2[1]$ and, *e.g.*, $\text{H}_3\text{C}-\text{I}$ can convincingly be rationalized by assuming a nucleophilic pathway, the possible operation of a radical mechanism remains to be ruled out. We first note in this context that 1,2-dihaloethane in the presence of $\text{Li}_2[1]$ did not undergo reductive dehalogenation with ethene formation. Yamashita, Nozaki *et al.* have treated their boryllithium compound with methyl trifluoromethanesulfonate (H_3COTf)⁴² on the one hand and benzyl bromide (BnBr) on the other (Scheme 10, top). In the first case, they observed the corresponding methyl borane in yields of 85%, whereas in the second case exclusively the bromoborane was obtained.⁴³ To explain the different outcomes, they proposed halogenophilic attack of the boryllithium or single electron transfer to the benzyl halide. We repeated Nozaki's

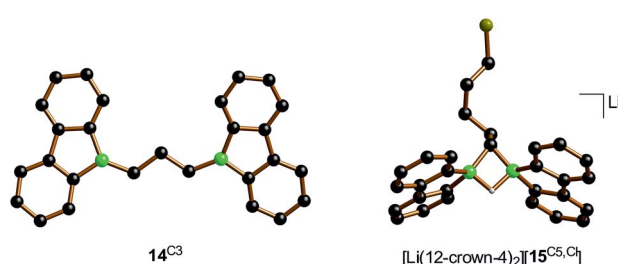
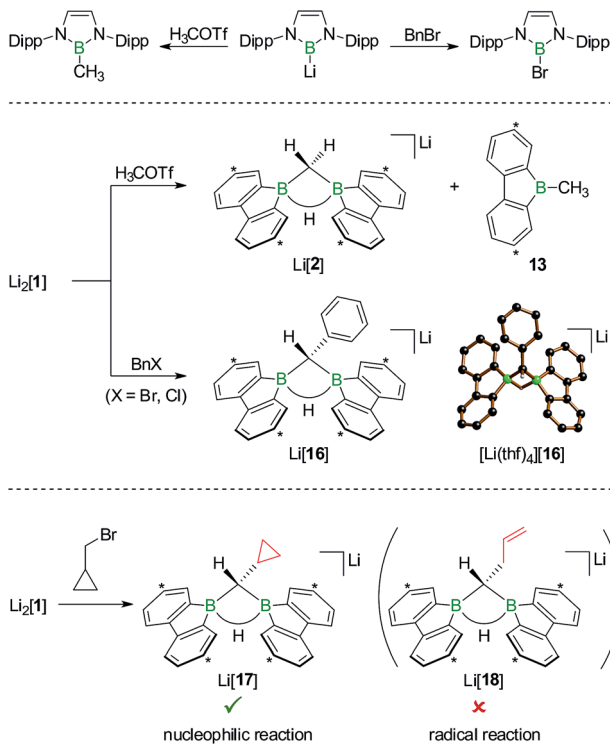


Fig. 4 Molecular structures of **14**^{C₃} and of the terminally chlorine-substituted $[\text{Li}(\text{12-crown-4})_2][15^{\text{C}5,\text{Cl}}]$ in the solid state. The solvent-separated $[\text{Li}(\text{12-crown-4})_2]^+$ cation, all *t*Bu groups, and all CH atoms are omitted for clarity.

Yamashita, Nozaki 2008

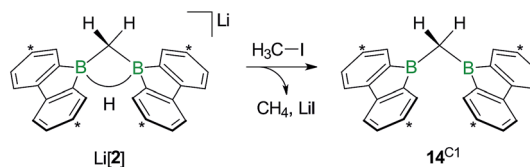


Scheme 10 The reactions of Yamashita's and Nozaki's boryllithium compound with H_3COTf or BnBr furnish the corresponding methyl borane or bromoborane, respectively (top). In the analogous reactions with $\text{Li}_2[1]$, only the organyl moieties are transferred to boron (middle; cf. $\text{Li}[2]/13$ and $\text{Li}[16]$). The reaction of $\text{Li}_2[1]$ with the radical clock (bromomethyl)cyclopropane quantitatively furnishes $\text{Li}[17]$, which is a strong indication for a closed-shell, nucleophilic pathway (bottom). $\text{Dipp} = 2,6-(i\text{Pr})_2\text{C}_6\text{H}_3$, $\text{Bn} = \text{CH}_2\text{C}_6\text{H}_5$, $\text{H}_3\text{COTf} = \text{H}_3\text{COSO}_2\text{CF}_3$; carbon atoms marked with asterisks bear $t\text{Bu}$ substituents. In the crystal structure plot of $[\text{Li}(\text{thf})_4][16]$, the solvent-separated cation, the $t\text{Bu}$ groups, and all $\text{C}(\text{sp}^2)-\text{H}$ atoms are omitted for clarity.

experiments with $\text{Li}_2[1]$ (Scheme 10, middle): H_3COTf showed the same reactivity as described above for $\text{H}_3\text{C-I}$ (cf. $\text{Li}[2]$ and 13); BnBr (as well as BnCl) gave the C–H-activation product $\text{Li}[16]$ rather than any haloboranes, as confirmed by NMR spectroscopy and X-ray crystallography on $[\text{Li}(\text{thf})_4][16]$.

As the ultimate test, we added $\text{Li}_2[1]$ to 1 equiv. of (bromomethyl)cyclopropane, a well-established radical clock (Scheme 10, bottom).^{44–46} A quantitative conversion to the C–H-activation product $\text{Li}[17]$, still carrying an intact cyclopropyl substituent, occurred (NMR-spectroscopic control). The absence of the ring-opened olefin derivative $\text{Li}[18]$ in the reaction mixture strongly supports the proposal of a closed-shell scenario in contrast to an open-shell process.

The results collected thus far are not only fundamentally interesting with respect to the reactivities of electron-rich $\text{B}=\text{B}$ double bonds, but open new access routes to ditopic boranes of high Lewis acidity. Molecules containing two or more potentially cooperating boron sites are of great current interest, *inter alia*, as organocatalysts^{5,11,47} or electron-storage media.^{48,49} Compounds of the class 14^{Cn} already constitute free Lewis



Scheme 11 The addition of $\text{H}_3\text{C-I}$ to $\text{Li}[2]$ furnishes the bis(9-borafluorenyl)methane $14^{\text{C}1}$. Carbon atoms marked with asterisks bear $t\text{Bu}$ substituents.

acids, but do not contain functional groups amenable to further derivatization.

The opposite is true for the salts $\text{Li}[15^{\text{Cn},\text{X}}]$. Here, the terminal halogen atoms provide ample opportunities, *e.g.*, for grafting the organoboron units onto polymers, dendrimers, or surfaces, but the Lewis acids need to be activated through LiH elimination prior to use.

While the bulky hydride scavenger $(\text{H}_3\text{C})_3\text{SiCl}$ failed in this respect, the smaller electrophile $\text{H}_3\text{C-I}$ efficiently transformed the model compound $\text{Li}[2]$ to its conjugate acid $14^{\text{C}1}$ (Scheme 11). As important diagnostic criteria, the BHB proton resonance vanishes in the course of the reaction, and the ^{11}B NMR signal shifts from the tetracoordinate ($\text{Li}[2]: \delta -14$ ppm) to the tricoordinate spectral region ($14^{\text{C}1}: \delta 45$ ppm).^{49,50}

In line with the reaction $\text{H}_3\text{C-I/Li}[2]$, the haloalkyl derivatives $\text{Li}[15^{\text{Cn},\text{X}}]$ are not long-term stable in THF at room temperature: ^1H NMR monitoring of the solutions revealed in each case a gradual decrease of the CH_2X resonance and a concomitant increase of a signal assignable to a terminal CH_3 group, which leads to the conclusion that the pending haloalkyl substituent can take a similar role as added $\text{H}_3\text{C-I}$. It is important to note in this context that the follow-up X/H exchange reactions are completely suppressed at -78°C and even at room temperature slow enough not to interfere with targeted derivatizations of the CH_2X termini.

Conclusion

In summary, $\text{C}(\text{sp}^3)-\text{H}$ activation and nucleophilic substitution reactions have been performed on the same redox-active diborane platform. We propose that the doubly 2,2'-biphenylene-bridged diborane(6) 1H_2 reacts with H_3CLI to furnish the rearranged $\text{B}(\text{sp}^2)-\text{B}(\text{sp}^3)$ intermediate $\text{Li}[\text{FluB-BFlu}(\text{CH}_3)]$ ($\text{Li}[6]$; BFlu = 9-borafluorenyl). $\text{Li}[6]$ also forms *via* an umpolung approach starting from H_3CX and the $\text{B}=\text{B}$ bonded, nucleophilic $\text{Li}_2[1]$, a compound which can be regarded as the product of a double deprotonation of 1H_2 ($\text{X} = \text{Cl}, \text{I}$). $\text{Li}[6]$ readily undergoes B–B-bond heterolysis to formally give the $[\text{BFlu}]^-$ anion and $(\text{H}_3\text{C})\text{BFlu}$ (13). The final product distribution depends on the relative amount of H_3CX and the leaving-group qualities of X , because $[\text{BFlu}]^-$ can either insert into a $\text{C}(\text{sp}^3)-\text{H}$ bond of 13 or replace the halogen atom of a second equivalent of H_3CX . The product of the carbene-type C–H insertion is $\text{Li}[\text{FluB}(\mu\text{-CH}_2)(\mu\text{-H})\text{BFlu}]$ ($\text{Li}[2]$) while the nucleophilic substitution on C–X generates 2 equiv. of 13 . Further insight into the competition between the two scenarios was

gained with the help of α,ω -dihaloalkanes $X(CH_2)_nX$ ($X = Cl, Br$). In the resulting intermediates $Li[FluB-BFlu((CH_2)_nX)]$, both possible follow-up reactions should be intramolecular processes. A longer alkylidene chain corresponds to a lower local concentration of the electrophile, while the BCH_2 groups are always similarly close to the reactive B–B bond. Consequently, short chains ($n = 2,3$) result in double substitution products $FluB(CH_2)_nBFlu$ and long chains ($n = 5,6$) in C–H-activation products $Li[FluB(\mu-C(H)(CH_2)_{n-1}X)(\mu-H)BFlu]$. In the case of the intermediate chain length $n = 4$, a mixture of both compounds is obtained: the worse leaving group $X = Cl$ leads to a higher proportion of the C–H-activated species, the better leaving group $X = Br$ furnishes more $FluB(CH_2)_4BFlu$. We finally note that the B–B-bond heterolysis of $Li[6]$ with concomitant transfer of a reactive $[BFlu]^-$ moiety is reminiscent of the reactivity patterns of the widely used alkoxy-diborane(4) adducts $[pinB-Bpin(OR)]^-$.²⁵ As a decisive difference, however, $[BFlu]^-$ appears to be considerably more reactive than *in situ*-generated $[Bpin]^-$, because C–H-insertion reactions of the latter are so far unknown.

Conflicts of interest

There are no conflicts to declare.

Acknowledgements

T. K. thanks the Fonds der Chemischen Industrie for a Ph.D. grant. The authors are grateful to Dr M. Diefenbach for helpful discussions regarding the quantum-chemical calculations. We acknowledge Prof. E. D. Jemmis and Sagar Ghorai for discussions. We thank Albemarle Lithium GmbH (Frankfurt) for the generous gift of chemicals. Credit for the TOC-background picture: European Southern Observatory, ESO/L. Calçada.

Notes and references

- 1 *Organoboranes for Syntheses*, ed. P. V. Ramachandran and H. C. Brown, American Chemical Society, ACS Symposium Series, Washington D.C., 2001.
- 2 N. Miyaura and A. Suzuki, *Chem. Rev.*, 1995, **95**, 2457–2483.
- 3 S. N. Kessler and H. A. Wegner, *Org. Lett.*, 2010, **12**, 4062–4065.
- 4 J. B. Grande, T. Urlich, T. Dickie and M. A. Brook, *Polym. Chem.*, 2014, **5**, 6728–6739.
- 5 L. Schweighauser and H. A. Wegner, *Chem.-Eur. J.*, 2016, **22**, 14094–14103.
- 6 E. von Grotthuss, A. John, T. Kaese and M. Wagner, *Asian J. Org. Chem.*, 2018, **7**, 37–53.
- 7 *Frustrated Lewis Pairs I & II*, ed. G. Erker and D. W. Stephan, Springer, Heidelberg, 2013.
- 8 D. W. Stephan and G. Erker, *Angew. Chem., Int. Ed.*, 2015, **54**, 6400–6441.
- 9 D. W. Stephan, *Science*, 2016, **354**, aaf7229.
- 10 A. Lorbach, M. Bolte, H.-W. Lerner and M. Wagner, *Organometallics*, 2010, **29**, 5762–5765.

- 11 E. von Grotthuss, M. Diefenbach, M. Bolte, H.-W. Lerner, M. C. Holthausen and M. Wagner, *Angew. Chem., Int. Ed.*, 2016, **55**, 14067–14071.
- 12 (a) A. Hübner, M. Bolte, H.-W. Lerner and M. Wagner, *Angew. Chem., Int. Ed.*, 2014, **53**, 10408–10411; (b) A. Hübner, A. M. Diehl, M. Bolte, H.-W. Lerner and M. Wagner, *Organometallics*, 2013, **32**, 6827–6833.
- 13 T. Kaese, A. Hübner, M. Bolte, H.-W. Lerner and M. Wagner, *J. Am. Chem. Soc.*, 2016, **138**, 6224–6233.
- 14 T. Kaese, H. Budy, M. Bolte, H.-W. Lerner and M. Wagner, *Angew. Chem., Int. Ed.*, 2017, **56**, 7546–7550.
- 15 K. M. Waltz and J. F. Hartwig, *Science*, 1997, **277**, 211–213.
- 16 A. E. Shilov and G. B. Shul'pin, *Chem. Rev.*, 1997, **97**, 2879–2932.
- 17 K. M. Waltz and J. F. Hartwig, *J. Am. Chem. Soc.*, 2000, **122**, 11358–11369.
- 18 I. A. M Khalid, J. H. Barnard, T. B. Marder, J. M. Murphy and J. F. Hartwig, *Chem. Rev.*, 2010, **110**, 890–931.
- 19 (a) P. Bissinger, H. Braunschweig, A. Damme, R. D. Dewhurst, T. Kupfer, K. Radacki and K. Wagner, *J. Am. Chem. Soc.*, 2011, **133**, 19044–19047. Related examples include: (b) T. Mennekes, P. Paetzold and R. Boese, *Angew. Chem., Int. Ed.*, 1990, **29**, 899–900; (c) W. J. Grigsby and P. P. Power, *J. Am. Chem. Soc.*, 1996, **118**, 7981–7988; (d) W. J. Grigsby and P. P. Power, *Chem.-Eur. J.*, 1997, **3**, 368–375; (e) Y. Wang and G. H. Robinson, *Inorg. Chem.*, 2011, **50**, 12326–12337; (f) D. P. Curran, A. Boussonnière, S. J. Geib and E. Lacôte, *Angew. Chem., Int. Ed.*, 2012, **51**, 1602–1605; (g) Y.-L. Rao, L. D. Chen, N. J. Mosey and S. Wang, *J. Am. Chem. Soc.*, 2012, **134**, 11026–11034.
- 20 L. Wang, Y. Fang, H. Mao, Y. Qu, J. Zuo, Z. Zhang, G. Tan and X. Wang, *Chem.-Eur. J.*, 2017, **23**, 6930–6936.
- 21 (a) É. Rochette, M.-A. Courtemanche and F.-G. Fontaine, *Chem.-Eur. J.*, 2017, **23**, 3567–3571. Related examples include: (b) G. Ménard and D. W. Stephan, *Angew. Chem., Int. Ed.*, 2012, **51**, 4409–4412; (c) G. Ménard, J. A. Hatnean, H. J. Cowley, A. J. Lough, J. M. Rawson and D. W. Stephan, *J. Am. Chem. Soc.*, 2013, **135**, 6446–6449.
- 22 The following literature survey focuses entirely on free boron-centered nucleophiles and does not cover corresponding transition-metal complexes. For an overview of these and related compound classes, see: (a) H. Braunschweig and T. Wagner, *Angew. Chem., Int. Ed.*, 1995, **34**, 825–826; (b) H. Braunschweig, M. Burzler, R. D. Dewhurst and K. Radacki, *Angew. Chem., Int. Ed.*, 2008, **47**, 5650–5653; (c) T. Kajiwara, T. Terabayashi, M. Yamashita and K. Nozaki, *Angew. Chem., Int. Ed.*, 2008, **47**, 6606–6610; (d) H. Braunschweig, R. D. Dewhurst, T. Herbst and K. Radacki, *Angew. Chem., Int. Ed.*, 2008, **47**, 5978–5980; (e) T. Terabayashi, T. Kajiwara, M. Yamashita and K. Nozaki, *J. Am. Chem. Soc.*, 2009, **131**, 14162–14163; (f) H. Braunschweig, P. Brenner, R. D. Dewhurst, M. Kaupp, R. Müller and S. Östreich, *Angew. Chem., Int. Ed.*, 2009, **48**, 9735–9738; (g) Y. Segawa, M. Yamashita and K. Nozaki, *Angew. Chem., Int. Ed.*, 2007, **46**, 6710–6713; (h) A. Steffen, R. M. Ward, W. D. Jones and T. B. Marder, *Coord. Chem. Rev.*, 2010, **254**, 1950–1976; (i) R. Frank,





J. Howell, J. Campos, R. Tirfoin, N. Phillips, S. Zahn, D. M. P. Mingos and S. Aldridge, *Angew. Chem., Int. Ed.*, 2015, **54**, 9586–9590; (f) H. Braunschweig, J. O. C. Jimenez-Halla, K. Radacki and R. Shang, *Chem. Commun.*, 2015, **51**, 16569–16572.

23 (a) Y. Segawa, M. Yamashita and K. Nozaki, *Science*, 2006, **314**, 113–115; (b) Y. Segawa, Y. Suzuki, M. Yamashita and K. Nozaki, *J. Am. Chem. Soc.*, 2008, **130**, 16069–16079; (c) M. Soleilhavoup and G. Bertrand, *Angew. Chem., Int. Ed.*, 2017, **56**, 10282–10292; (d) L. Weber, *Eur. J. Inorg. Chem.*, 2017, 3461–3488. Related examples include: (e) M. Unverzagt, G. Subramanian, M. Hofmann, P. von Ragué Schleyer, S. Berger, K. Harms, W. Massa and A. Berndt, *Angew. Chem., Int. Ed.*, 1997, **36**, 1469–1472; (f) S. Robinson, J. McMaster, W. Lewis, A. J. Blake and S. T. Liddle, *Chem. Commun.*, 2012, **48**, 5769–5771; (g) W. Lu, H. Hu, Y. Li, R. Ganguly and R. Kinjo, *J. Am. Chem. Soc.*, 2016, **138**, 6650–6661; (h) B. Wang, Y. Li, R. Ganguly, H. Hirao and R. Kinjo, *Nat. Commun.*, 2016, **7**, 11871; (i) M. M. Morgan, J. M. Rautiainen, W. E. Piers, H. M. Tuononen and C. Gendy, *Dalton Trans.*, 2018, **47**, 734–741.

24 (a) A.-F. Pécharman, A. L. Colebatch, M. S. Hill, C. L. McMullin, M. F. Mahon and C. Weetman, *Nat. Commun.*, 2017, **8**, 15022; (b) A.-F. Pécharman, M. S. Hill, C. L. McMullin and M. F. Mahon, *Angew. Chem., Int. Ed.*, 2017, **56**, 16363–16366.

25 (a) C. Kleeberg, L. Dang, Z. Lin and T. B. Marder, *Angew. Chem., Int. Ed.*, 2009, **48**, 5350–5354; (b) R. D. Dewhurst, E. C. Neeve, H. Braunschweig and T. B. Marder, *Chem. Commun.*, 2015, **51**, 9594–9607; (c) S. Pietsch, E. C. Neeve, D. C. Apperley, R. Bertermann, F. Mo, D. Qiu, M. S. Cheung, L. Dang, J. Wang, U. Radius, Z. Lin, C. Kleeberg and T. B. Marder, *Chem.-Eur. J.*, 2015, **21**, 7082–7098; (d) E. C. Neeve, S. J. Geier, I. A. Mkhald, S. A. Westcott and T. B. Marder, *Chem. Rev.*, 2016, **116**, 9091–9161; (e) J. Cid, H. Gulyás, J. J. Carbó and E. Fernández, *Chem. Soc. Rev.*, 2012, **41**, 3558–3570.

26 (a) H. Braunschweig, C.-W. Chiu, K. Radacki and T. Kupfer, *Angew. Chem., Int. Ed.*, 2010, **49**, 2041–2044; (b) R. Bertermann, H. Braunschweig, R. D. Dewhurst, C. Hörl, T. Kramer and I. Krummenacher, *Angew. Chem., Int. Ed.*, 2014, **53**, 5453–5457. For an overview of *N*-heterocyclic carbene boranes, see: (c) D. P. Curran, A. Solovyev, M. Makhlof Brahmi, L. Fensterbank, M. Malacria and E. Lacôte, *Angew. Chem., Int. Ed.*, 2011, **50**, 10294–10317.

27 (a) R. Kinjo, B. Donnadieu, M. A. Celik, G. Frenking and G. Bertrand, *Science*, 2011, **333**, 610–613. Related examples include: (b) T. Imamoto and T. Hikosaka, *J. Org. Chem.*, 1994, **59**, 6753–6759; (c) J. Monot, A. Solovyev, H. Bonin-Dubarle, É. Derat, D. P. Curran, M. Robert, L. Fensterbank, M. Malacria and E. Lacôte, *Angew. Chem., Int. Ed.*, 2010, **49**, 9166–9169; (d) D. A. Ruiz, G. Ung, M. Melaimi and G. Bertrand, *Angew. Chem., Int. Ed.*, 2013, **52**, 7590–7592; (e) D. A. Ruiz, M. Melaimi and G. Bertrand, *Chem. Commun.*, 2014, **50**, 7837–7839; (f) L. Kong, Y. Li, R. Ganguly, D. Vidovic and R. Kinjo, *Angew. Chem., Int. Ed.*, 2014, **53**, 9280–9283; (g) L. Kong, R. Ganguly, Y. Li and R. Kinjo, *Chem. Sci.*, 2015, **6**, 2893–2902.

28 (a) E. Bernhardt, V. Bernhardt-Pitchouina, H. Willner and N. Ignat'ev, *Angew. Chem., Int. Ed.*, 2011, **50**, 12085–12088; (b) J. Landmann, J. A. P. Sprenger, R. Bertermann, N. Ignat'ev, V. Bernhardt-Pitchouina, E. Bernhardt, H. Willner and M. Finze, *Chem. Commun.*, 2015, **51**, 4989–4992; (c) J. Landmann, J. A. P. Sprenger, M. Hailmann, V. Bernhardt-Pitchouina, H. Willner, N. Ignat'ev, E. Bernhardt and M. Finze, *Angew. Chem., Int. Ed.*, 2015, **54**, 11259–11264; (d) H. Braunschweig, R. D. Dewhurst, L. Pentecost, K. Radacki, A. Vargas and Q. Ye, *Angew. Chem., Int. Ed.*, 2016, **55**, 436–440.

29 G. R. Fulmer, A. J. M. Miller, N. H. Sherden, H. E. Gottlieb, A. Nudelman, B. M. Stoltz, J. E. Bercaw and K. I. Goldberg, *Organometallics*, 2010, **29**, 2176–2179.

30 (a) L. Kaufmann, H. Vitze, M. Bolte, H.-W. Lerner and M. Wagner, *Organometallics*, 2008, **27**, 6215–6221; (b) A. Iida, A. Sekioka and S. Yamaguchi, *Chem. Sci.*, 2012, **3**, 1461–1466.

31 See ref. 25b.

32 M. Saunders and E. L. Hagen, *J. Am. Chem. Soc.*, 1968, **90**, 6881–6882.

33 G. A. Olah and A. M. White, *J. Am. Chem. Soc.*, 1969, **91**, 5801–5810.

34 G. A. Olah and A. M. White, *J. Am. Chem. Soc.*, 1969, **91**, 6883–6885.

35 L. Radom, J. A. Pople, V. Buss and P. v. R. Schleyer, *J. Am. Chem. Soc.*, 1972, **94**, 311–321.

36 P. C. Hariharan, L. Radom, J. A. Pople and P. v. R. Schleyer, *J. Am. Chem. Soc.*, 1974, **96**, 599–601.

37 M. Saunders, P. Vogel, E. L. Hagen and J. Rosenfeld, *Acc. Chem. Res.*, 1973, **6**, 53–59.

38 H. Nöth and B. Wrackmeyer, *Nuclear Magnetic Resonance Spectroscopy of Boron Compounds*, in *NMR Basic Principles and Progress*, ed. P. Diehl, E. Fluck and R. Kosfeld, Springer Verlag, Berlin, Heidelberg, New York, 1978.

39 Scattered precedence for comparable reactivity of electron-precise B–B single and multiple bonds exists: (a) A. Hübner, T. Kaese, M. Diefenbach, B. Endeward, M. Bolte, H.-W. Lerner, M. C. Holthausen and M. Wagner, *J. Am. Chem. Soc.*, 2015, **137**, 3705–3714; (b) H. Braunschweig, P. Constantinidis, T. Dellermann, W. C. Ewing, I. Fischer, M. Hess, F. R. Knight, A. Rempel, C. Schneider, S. Ullrich, A. Vargas and J. D. Woollins, *Angew. Chem., Int. Ed.*, 2016, **55**, 5606–5609; (c) M. Frick, E. Kaifer and H.-J. Himmel, *Angew. Chem., Int. Ed.*, 2017, **56**, 11645–11648; (d) M. Arrowsmith, H. Braunschweig and T. E. Stennett, *Angew. Chem., Int. Ed.*, 2017, **56**, 96–115; (e) A. Widera, E. Kaifer, H. Wadebold and H.-J. Himmel, *Chem.-Eur. J.*, 2018, **24**, 1209–1216; (f) J. Horn, A. Widera, S. Litters, E. Kaifer and H.-J. Himmel, *Dalton Trans.*, 2018, **47**, 2009–2017.

40 A comparable selectivity toward C–H activation was also observed for EtBr (cf. Li[19] in the ESI†).

41 T. Kaese, T. Trageser, H. Budy, M. Bolte, H.-W. Lerner and M. Wagner, 2018, Private communication to the

Cambridge Structural Database; deposition numbers: CCDC 1819625 ($[\text{Li}(\text{thf})_4][\text{Li}^{15\text{C}4,\text{Cl}}]\cdot\text{THF}$), CCDC 1819626 ($[\text{Li}(\text{thf})_4][\text{Li}^{15\text{C}6,\text{Cl}}]\cdot\text{THF}$), and CCDC 1819627 ($[\text{Li}(\text{thf})_4][\text{Li}^{15\text{C}6,\text{Br}}]$).†

42 S. J. Tremont and H. U. Rahman, *J. Am. Chem. Soc.*, 1984, **106**, 5759–5760.

43 See ref. 23b.

44 D. Griller and K. U. Ingold, *Acc. Chem. Res.*, 1980, **13**, 317–323.

45 D. C. Nonhebel, *Chem. Soc. Rev.*, 1993, **22**, 347–359.

46 C. Chen, L. Ouyang, Q. Lin, Y. Liu, C. Hou, Y. Yuan and Z. Weng, *Chem.-Eur. J.*, 2014, **20**, 657–661.

47 A. Lorbach, M. Bolte, H.-W. Lerner and M. Wagner, *Chem. Commun.*, 2010, **46**, 3592–3594.

48 A. Hübner, A. M. Diehl, M. Diefenbach, B. Endeward, M. Bolte, H.-W. Lerner, M. C. Holthausen and M. Wagner, *Angew. Chem., Int. Ed.*, 2014, **53**, 4832–4835.

49 See ref. 39a.

50 A. Hübner, Z.-W. Qu, U. Englert, M. Bolte, H.-W. Lerner, M. C. Holthausen and M. Wagner, *J. Am. Chem. Soc.*, 2011, **133**, 4596–4609.

